Development of Quenched Phase-Separated Structure in Poly(styrene-co-acrylonitrile)/Poly(methyl methacrylate) Blend under Elongational Flow

ARTICLE *in* MACROMOLECULES · OCTOBER 2000

Impact Factor: 5.8 · DOI: 10.1021/ma000358f

3 AUTHORS, INCLUDING:

Masami Okamoto
Toyota Technological Institute
124 PUBLICATIONS **10,951** CITATIONS

Macromolecules

Volume 33, Number 22 October 31, 2000

Communications to the Editor

Development of Quenched Phase-Separated Structure in Poly(styrene-*co*-acrylonitrile)/ Poly(methyl methacrylate) Blend under Elongational Flow

Yong Hoon Kim, Masami Okamoto, and Tadao Kotaka*

Advanced Polymeric Materials Engineering, Graduate School of Engineering, Toyota Technological Institute, Hisakata 2-12-1, Tempaku, Nagoya 468-8511, Japan

Received February 28, 2000
Revised Manuscript Received May 23, 2000

In our previous paper,[1] we described structural change induced by elongational flow with constant Hencky strain rate $\dot{\epsilon}_0$ in poly(styrene-*co*-acrylonitrile) (SAN)/ poly(methyl methacrylate) (PMMA) blend of near-critical composition (40/60 w/w) *above* its lower critical solution temperature (LCST: T_s = 195 °C) where spinodal decomposition (SD) proceeded during the elongation as well as *below* its T_s, where the blend was a miscible one-phase system. In the study we employed *elongational flow optorheometry* (EFOR)[2] developed for the simultaneous monitoring of time development of *transient* tensile stress $\sigma(\dot{\epsilon}_0;t)$ and birefringence $\Delta n(\dot{\epsilon}_0;t)$ in polymer melts under elongation with constant strain rates $\dot{\epsilon}_0$. In particular, we examined the validity of the stress optical rule (SOR)[2−4] for the elongation of the blend. In the miscible, one-phase state at 150 °C, the SOR was valid, and the observed stress optical coefficient $C(\dot{\epsilon}_0;t)$ [$\equiv\Delta n(\dot{\epsilon}_0;t)/\sigma(\dot{\epsilon}_0;t)$] was a constant $C_{\text{blend}} = -1.2 \times 10^{-9}$ Pa^{-1} dependent neither on $\dot{\epsilon}_0$, Hencky strain ϵ ($\equiv \dot{\epsilon}_0 \cdot t$), nor tensile stress $\sigma(\dot{\epsilon}_0;t)$. On the other hand, the SOR was clearly violated for the blend undergoing SD at 215 °C where competitive coarsening of the domain structure took place due both to SD and elongation. The C_{blend} changed its sign from negative to positive in the early stage, and the value of C_{blend} increased as the morphology of the phase-separated structure constantly changed in the intermediate-to-late stage of elongation.[1]

We thus designed a new experiment to distinguish the effects of SD and of elongation on the morphology development in the SAN/PMMA blend. We examined the blend, which was first phase-separated above T_s (=195 °C) up to a certain SD time under a quiescent state, quenched to room temperature to freeze the domain morphology, and then subjected the blend to elongation at 150 °C well below T_s, where further domain coarsening due to SD hardly proceeded.

The SAN/PMMA blend with near critical composition of 40/60 (w/w) was annealed at 215 or 220 °C for 10 min in a temperature-controlled hot stage and then quenched to room temperature to freeze the structure. The annealing conditions corresponded to the *reduced* SD time $\tau = 5.0$ for the former and $\tau = 8.0$ for the latter with τ being defined by the linearized Cahn−Hilliard theory[5] of SD. The blends were in the intermediate stage of SD at the start of the elongation.

In each run, a specimen was first annealed for 60 s on the sample stage of EFOR kept at 150 °C to equilibrate the temperature and then stretched with a nominal strain rate between 0.001 and 1.0 s^{-1}. The real strain rate $\dot{\epsilon}_0$ effective to the sample was estimated from the decrease in the width of the sample during elongation,[6] and the corrected values were found to be 0.000 98 for the nominal 0.001 s^{-1} and 0.93 for the nominal 1.0 s^{-1} elongation. At a certain stage of elongation the specimen was taken out from EFOR and rapidly quenched by placing it between cold metal plates to freeze the internal structure. The recovered sample of approximately 100 μm thickness was subjected to light scattering (LS) measurement[7] under the Vv scattering mode and to optical microscopy (OM) observation. Then microtomed thin sections (of ca. 100 nm thickness) of the recovered sample stained with ruthenium tetraoxide (RuO_4) were subjected to transmission electron microscopy (TEM) observation. For analyzing the features of these micrographs, we carried out fast Fourier transform (FFT) analysis on digitally saved images of both

* To whom correspondence should be addressed. Tel +81-52-809-1860; FAX +81-52-809-1864; E-mail kotaka@toyota-ti.ac.jp.

10.1021/ma000358f CCC: $19.00
Published on Web 10/11/2000

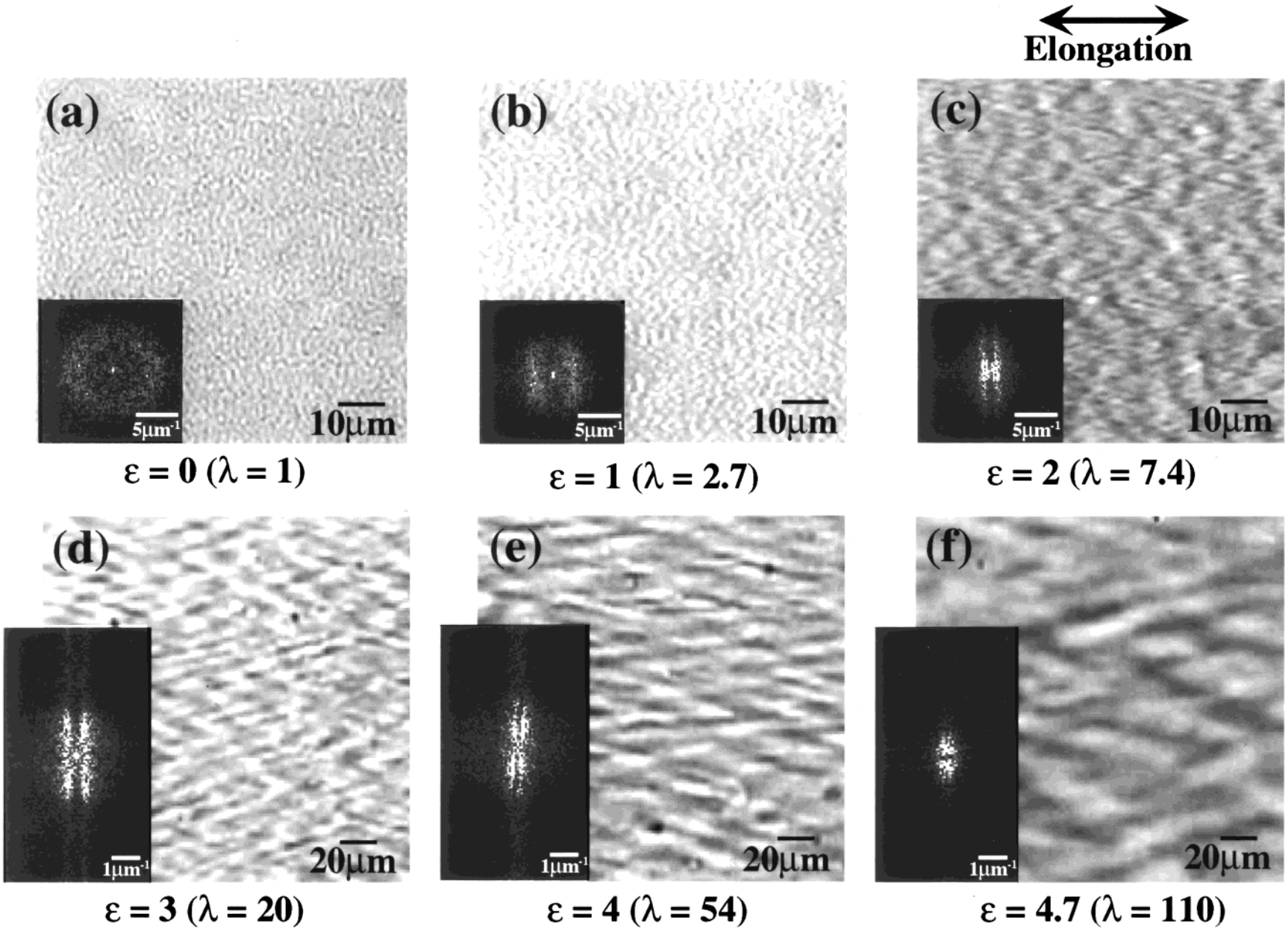

Figure 1. OM micrographs showing a frozen phase-separated structure ($\tau = 8.0$) of SAN/PMMA (40/60) blend (a) before elongation ($\epsilon = 0$) and elongated at 150 °C with $\dot{\epsilon}_0 = 0.93$ s^{-1} up to (b) $\epsilon = 1.0$, (c) 2.0, (d) 3.0, (e) 4.0, and (f) 4.7. The inset in each picture is a computed fast Fourier transform (FFT) spectrrum of the micrograph.

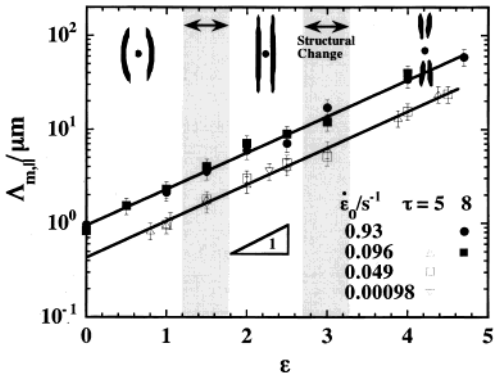

Figure 2. Semilogarithmic plots of characteristic length $\Lambda_{m,||}$ for elongational direction vs Hencky strain ϵ of a frozen phase-separated structure (τ = 5.0 and 8.0) of SAN/PMMA (40/60) blend elongated at 150 °C for four different strain rate ϵ_0 (=0.000 98−0.93 s^{-1}). The two gray zones represent a region of structural change analyzed by LS experimant and FFT spectra.

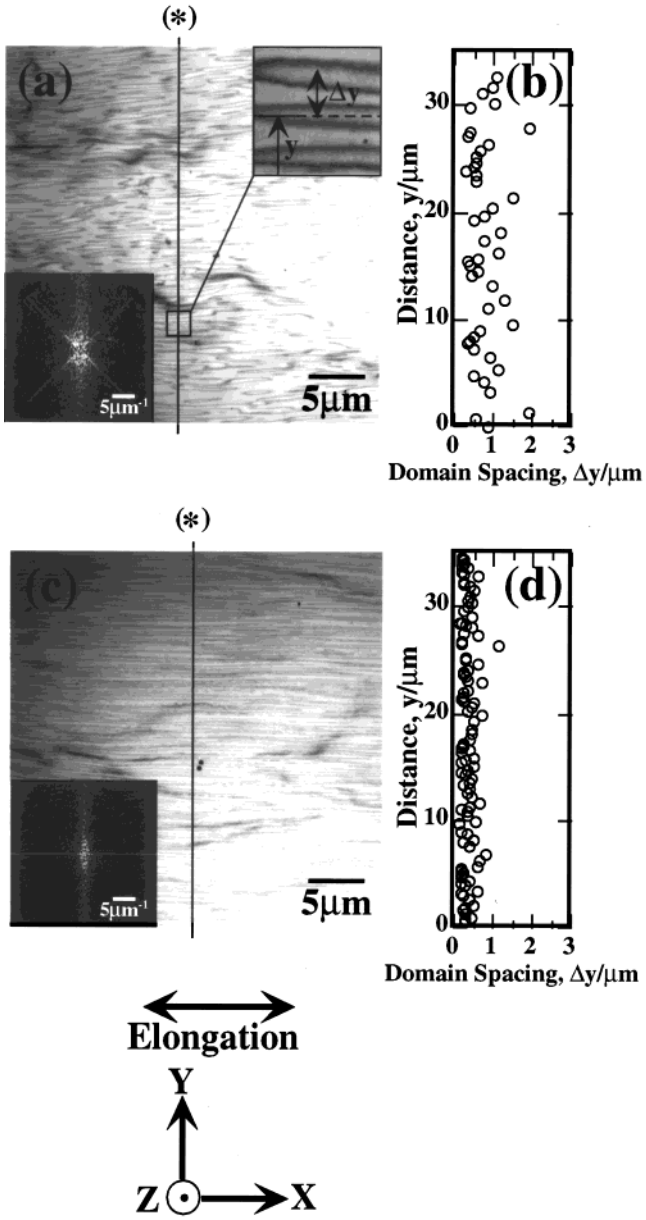

Figure 3. TEM pictures and plots of position vs domain spacing for SAN/PMMA (40/60) blend with a frozen phase-separated (τ = 8.0) structure elongated at 150 °C with $\dot{\epsilon}_0$ = 0.93 s^{-1} up to (a, b) ϵ = 2 and (c, d) 4.

OM and TEM micrographs, using commercial image analysis software (Ultimage, Graftek, France), which allowed to provide us information equivalent to the scattering analyses.

Figure 1a−f shows a series of OM photographs with their FFT patterns of the SAN/PMMA blend quenched from the intermediate stage (τ = 8.0) of SD and elongated at 150 °C with $\dot{\epsilon}_0$ = 0.93 s^{-1} up to various ϵ from 0 up to 4.7. Figure 1a is for the blend before elongation (ϵ = 0), in which we see an bicontinuous structure and a ringlike FFT pattern (halo). This picture implies that the morphology of the blend before elongation (ϵ = 0) is isotropic. Figure 1b is the OM photograph with its FFT spectrum for the blend elongated up to ϵ = 1.0. The FFT pattern shows a so-called *two-wing* pattern with the maximum intensity in the meridional direction. This suggests that in the OM photographs the correlation has disappeared in the perpendicular direction with increasing ϵ, but the domains become somewhat ordered along the stretch direction. As ϵ is further increased, a *zigzag* pattern appears at around ϵ = 2 (Figure 1c) and grows continuously up to 4.7 (Figure 1f). The FFT spectra transform from a two-wing pattern to a *four-spot-like* pattern, accompanying an increase in the intensity (cf. Figure 1c−f). The results imply that the ordering appears along the perpendicular direction as well. The behavior is more or less the same for the blend elongated with different strain rates. The development is governed essentially by the Hencky strain ϵ and rather insensitive to the strain rates $\dot{\epsilon}_0$.

In Figure 2, the results of OM and LS observations are summarized for the two blends having the frozen phase-separated structure corresponding to the SD time of τ = 5.0 and τ = 8.0. The interdomain spacings $\Lambda_{m,||}$ of the two-wing or four-spot-like patterns in the direction parallel to the stretch direction are determined from the scattering vector q_m at the scattering maximum in the LS profiles and plotted in the figure against ϵ in the semilogarithmic scale. The LS $\Lambda_{m,||}$ values are in good agreement with those determined from the FFT spectra of the OM pictures.

The dependence of ln($\Lambda_{m,||}$) on ϵ is essentially the same for the blend annealed at 215 °C for 10 min (τ = 5.0) and for the blend at 220 °C for 10 min (τ = 8) annealing, except the front factor $\Lambda_{m,||}(\epsilon=0)$, obviously reflecting the difference in the SD structure at the start of elongation. In both cases, the plots for different $\dot{\epsilon}_0$ appear to conform a straight line with the slope of about 0.89, which implies the elongation is *nonaffine* due presumably to the absence of the direct coherency with bulk strain. Interestingly, despite the structure transformation taking place during the elongation, the $\Lambda_{m,||}$ is scaled with only one parameter, ϵ, up to very large deformation (ϵ = 4.7 or λ = 110). Recently, from OM and LS studies Weiss and co-workers[8] reported development of a unique *chevronlike* pattern in a near-critical SAN/PMMA blend under shear flow at 180 °C (T_s + 12 °C) with a shear rate of 0.02 s^{-1}. The OM photographs and their FFT spectra of our SAN/PMMA blend subjected to elongation also exhibit *chevronlike* patterns (cf. Figure 2c−f) with the features similar to those suggested by Weiss and co-workers.[8]

Then, a question arises: What morphology change do such unique chevronlike patterns represent? For elucidating the features of the structural change, we conducted TEM observation on the elongated blend specimens. Figure 3 shows two examples of the TEM picture

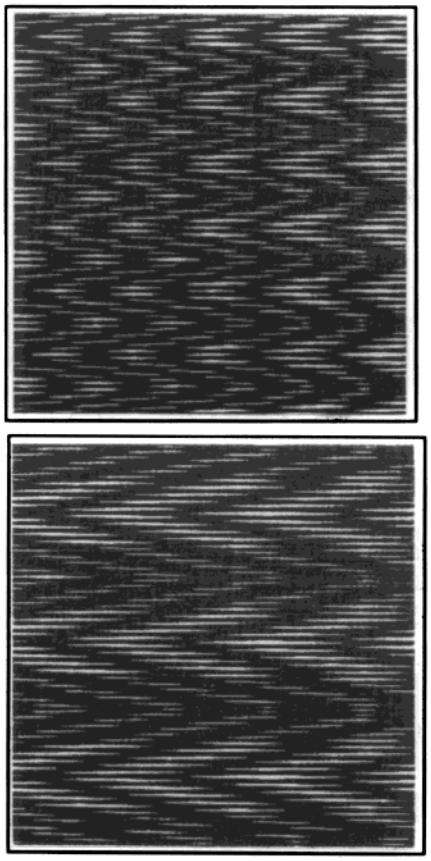

Figure 4. Simulated chevronlike pattern from a proposed superposition model. The simulation was made by superposition of two line lattices of the line width and the separation with the angle of inclination 5° (left) and 3° (right).

with the FFT pattern on the frozen phase-separated ($\tau = 8.0$) blend specimen elongated with $\dot{\epsilon}_0 = 1.0\ s^{-1}$ up to (a) $\epsilon = 2$ and (c) $\epsilon = 4$. Plots b and d show the domain spacings Δy along the perpendicular direction y (indicated with (*) line), determined directly from the TEM picture as illustrated in the inset of Figure 3a. In Figure 3a for the micrograph at $\epsilon = 2$, we see elongated domains along the stretching direction with the domain spacings ranging from 0.5 to 2 μm, as seen in Figure 3b. With increasing ϵ up to 4, we see highly elongated *fibillar* domains with the domain spacings below 1 μm. The average value of Δy and its dispersion becomes smaller with increasing ϵ (Figure 3c,d). We confirmed that this behavior is essentially the same at any other places of the micrograph. It is interesting to note that the TEM picture shows elongated fibrillar domains, while the OM picture exhibits a zigzag pattern (cf. Figure 1c vs 3a and Figure 1e vs 3c). Such a difference should have resulted, first of all, from the difference in thickness of the specimens subjected to OM (110 μm at $\epsilon = 2$, 40 μm at $\epsilon = 4$) and TEM (0.1 μm) observations.

For explaining this remarkable difference of the zigzag versus the fibrillar development between the thick versus thin specimens, we propose a superimposition model, which assumes that the former is composed of 400−1000 layers of the latter each composed of aligned fibrils of PS domains with different spacings and tiltings. The unique chevron patterns seen in Figure 1 may be caused if the axes of the fibrils are slightly tilted from one layer to the other and if the domain spacing is more or less nonuniform. Figure 4 shows two such examples of the model: The left panel shows the model of a weak correlation and a large tilting angle corresponding to the early stage of elongation (Figure 1c), and the right panel shows the model of a stronger correlation and a small tilting angle corresponding to the late stage of elongation (Figure 1e). The size of the zigzag (chevron) pattern in Figure 1 increases with decreasing inclination and decreasing nonuniformity in the domain spacing, as ϵ increases. Thus, in the OM photograph we see just a shadow of the piled-up thin layers each composed of oriented fibrils.[9] Such a superimposition model is also known for interpretation of the moiré pattern caused by misalignment of the two crystals with slightly different lattice spacings.[10]

Acknowledgment. We thank Prof. Toshiaki Ougizawa and Dr. Tuneo Chiba, Tokyo Institute of Technology, for taking TEM pictures shown in Figure 3.

References and Notes

(1) Kim, Y. H.; Okamoto, M.; Kotaka, T. Abstract PPS-15 Annual Meeting, The Netherlands, 1999; p 22. Kim, Y. H.; Okamoto, M.; Kotaka, T.; Ougizawa, T.; Tchiba, T.; Inoue, T. *Polymer* **2000**, *41*, 4747.
(2) Kotaka, T.; Kojima, A.; Okamoto, M. *Rheol. Acta* **1997**, *36*, 646.
(3) Doi, M.; Edwards, S. F. *The Theory of Polymer Dynamics*; Clarendon Press: Oxford, 1986.
(4) Janeschitz-Kriegel, H. *Polymer Melt Rheology and Flow Birefringence*; Springer-Verlag: New York, 1983.
(5) Cahn, J. W.; Hilliard, J. E. *J. Chem. Phys.* **1958**, *28*, 258.
(6) Meissner, J.; Hoesttler, J. *Rheol. Acta* **1994**, *33* (No. 1), 1−21. Schulze, J. S.; Lodge, T. P.; Macosko, C. W. Personal communication, 1999. "A comparison of LLDPE extensional viscosity measurements from various RME rheometers": A report to the participants in the recent round-robin experiment, Sept 1999.
(7) Kubo, H.; Sato, H.; Okamoto, M.; Kotaka, T. *Polym. Commun.* **1998**, *39*, 501.
(8) Hong, Z.; Shaw, M. T.; Weiss, R. A. *Macromolecules* **1998**, *31*, 6211.
(9) Kim, Y. H.; Okamoto, M.; Kotaka, T. Manuscript in preparation.
(10) Wunderich, B. *Macromolecular Physics*; Academic Press: New York, 1973; Vol. 1.

MA000358F